Available online at www.sciencedirect.com
ScienceDirect
International Journal of Heat and Mass Transfer 50 (2007) 4286–4296
International Journal of HEAT and MASS TRANSFER
www.elsevier.com/locate/ijhmt

A quasi-3D analysis of the thermal performance of a flat heat pipe

G. Carbajal [a,*], C.B. Sobhan [b], G.P. "Bud" Peterson [c], D.T. Queheillalt [d], Haydn N.G. Wadley [d]

[a] University of Turabo, Department of Mechanical Engineering, PO Box 3030, Gurabo, PR 00778, USA
[b] National Institute of Technology, Center for Nanotechnology, Department of Mechanical Engineering, Calicut 673 601, India
[c] University of Colorado at Boulder, Boulder, CO 80309-0017, USA
[d] University of Virginia, Department of Materials Science and Engineering, 116 Engineers Way, PO Box 400745, Charlottesville, VA 22904, USA

Received 8 November 2006; received in revised form 29 January 2007
Available online 8 May 2007

Abstract

The thermal performance of a flat heat pipe thermal spreader has been described by a quasi-3D mathematical model and numerically modeled. An explicit finite volume method with under-relaxation was used for computations in the vapor phase. This was combined with a relatively small time step for the analysis. The physical problem consisted of an evaporator surface that was transiently heated non-uniformly for a short period of time and the heat source then removed. Then the system was cooled by natural convection and radiative heat transfer at the condenser region. The transient temperature distributions at the front and back of the heat spreader were obtained for different times during the transient period. The velocity distribution in the vapor core was also obtained. Due to the effect of phase change at the evaporator and condenser sides, a significant amount of energy is found to be absorbed and partially released during the transient heating and cooling processes. The numerical results indicate that advection and the high thermal diffusivity of the vapor phase accelerate the propagation of the temperature distribution in the vapor core, making it uniform during this process. The condenser temperature distribution was almost uniform at the end of the transient heating process. The transient temperature distribution on a solid aluminum plate was compared with the flat heat pipe results and indicated that the flat heat pipe successfully spread the heat uniformly at the condenser side of the structure.

Keywords: Flat heat pipe; Heat spreader; Transient process; A quasi-tridimensional approach

1. Introduction

Since the first basic heat pipe concept proposed by Gaugler [1], heat pipes have been widely applied to a variety of sometimes simple and more recently, quite complex designs for space and terrestrial applications. Originally heat pipes were designed for heat transfer applications in space vehicles [2–5], but their high effective thermal conductivity later led to applications in terrestrial systems as well [6]. The application of heat pipes as heat transport devices and thermal spreaders for thermal management of electronic systems and devices is also an important area of research and development [7–9].

As passive devices with the ability to work both in ambient as well as high temperatures, and terrestrial as well as non-gravitational fields, heat pipes have become a unique and versatile heat transfer medium with a wide range of physical sizes and applications. Investigations on the transient operation of heat pipes have been reported for various external operating conditions [10–16]. Chang et al. [10] presented a finite difference analysis for predicting the transient operating characteristics of low temperature heat pipes. In their analysis, the convection heat transfer in the wick was neglected, assuming pure conduction in the wick. A detailed transient liquid flow analysis of a homogeneous heat pipe wick operating at low temperature was

* Corresponding author. Tel.: +1 787 743 7979; fax: +1 787 744 5476.
E-mail address: gcarbajal1@suagm.edu (G. Carbajal).

0017-9310/$ - see front matter © 2007 Published by Elsevier Ltd.
doi:10.1016/j.ijheatmasstransfer.2007.01.057

Nomenclature

c	specific heat per unit volume, J/(m^3 K)
C_E	Ergun's constant, 0.55
F_B	force per unit volume (Eq. (3))
g	gravitational constant, m s^{-2}
h	convection heat transfer coefficient, W/(m^2 K)
H	flat heat pipe height, m
K	permeability, m^2
k	thermal conductivity, W/(m K)
L	flat heat pipe length, m
M	molecular weight, kg kmol^{-1}
P	pressure, Pa
Q	heat transfer, W
q''	heat flux, W m^{-2}
R	vapor gas constant, J/(kg K)
$\boldsymbol{R}$	thermal resistance, K W^{-1}
t	time, s
T	temperature, K
$\vec{V}$	velocity in vector form, m s^{-1}
W	flat heat pipe width, m
x	axial direction, axial distance, m
y	width direction, width, m
z	length direction, m

Greek symbols

Λ	constant, 0.35
ε	emissivity
μ	dynamic viscosity, N s/m^2
ρ	density, kg m^{-3}
σ	surface tension, N/m
σ_R	Stefan–Boltzmann constant, 5.67×10^{-8} W/(m^2 K^4)
$\hat{\sigma}$	accommodation factor
φ	porosity

Subscripts

eff	effective
f	fluid
i	liquid–vapor interface
in	input
m	mean
out	output
s	wall material
v	vapor
w	wick material
∞	ambient conditions

performed experimentally and analytically by Ambrose et al. [11]. They observed significant reductions in the wick's saturation at high heat loads, thus affecting the wick-flow properties. In this study the wall thickness and vapor core were not taken into account in the overall analysis. In order to avoid complicated and impractical vapor flow models, a 1D vapor flow coupled with the evaporation and condensation rates was used by Chang et al. [12] to predict the vapor pressure and temperature drops in a liquid metal heat pipe. Tournier et al. [13] assumed an isothermal condition in the liquid–vapor interface to develop a 2D heat pipe transient analysis model. The mass flow rate at the evaporator and condenser were assumed to be the same in this model. The numerical instabilities during the phase change were suppressed by employing a mushy-cell temperature of 2×10^{-8} K [14]. To simplify the numerical study of a transient heat pipe Zuo et al. [15] assumed a quasi steady state 1D approach for the vapor flow and a transient 2D conduction in the wall and the wick. Sobhan et al. [16] presented a computational analysis to study the transient analysis of a flat heat pipe, where an energy balance was applied to compute the mass flux at the liquid vapor interface. Vaddakan et al. [17] presented a transient analysis of a flat heat pipe for a uniform heat input. Carbajal et al. [18] performed a numerical study to handle the early transient processes in a flat heat pipe subjected to a non-uniform heat input, using a simplified expression for the velocity at the liquid–vapor interface. The literature does not indicate significant efforts to measure the transient temperature distributions at the condenser and evaporator surfaces of flat heat pipe structures subjected to non-uniform heating.

The present analysis is designed to determine the transient temperature distribution on the back (condenser) side of a flat plate heat pipe and a solid aluminum plate subjected to similar conditions, for a constant and non-uniform heat input, in order to compare the advantage of using the heat pipe as a heat spreader. A quasi-3D approach was used in the present analysis, to capture the distributions of the field variables and the effects of parametric variations in the flat heat pipe system as completely as possible, without utilizing a computationally complex fully 3D analysis. The working fluid used was distilled water.

2. Physical model and solution

2.1. The physical model

The model consists of a heat pipe spreader configured as a structurally efficient sandwich panel with the front face sheets acting as the evaporator and the back side as the condenser, as shown in Fig. 1. The center point of the front plane was chosen to be the origin for the Cartesian coordinate system used in the analysis. The height, length, and width of the flat heat pipe were 0.56 m, 0.56 m, and 0.064 m. The solid plate had the same height and length, but the width was 0.013 m.

Here, the distance between the evaporator and the condenser is much smaller compared to conventional heat

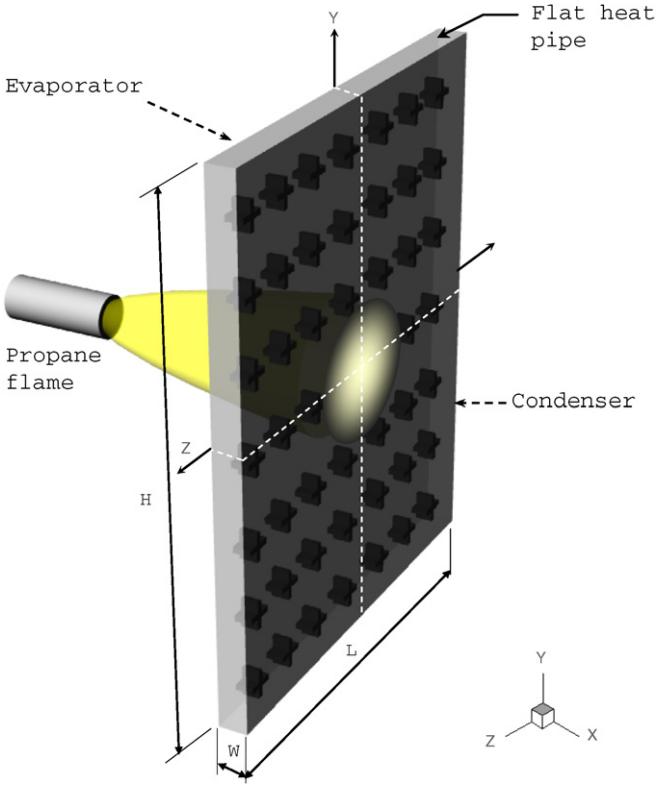

Fig. 1. Flat heat pipe with a localized thermal source applied to the evaporator side and a thermal imaging camera used to monitor the condenser surface temperature distribution.

pipes. In the analysis of such a system, the lateral sides (edges) and the top and bottom surfaces were assumed adiabatic, and a corresponding situation was used in the physical model. The temperature is ambient adjacent to the condenser side and is assumed to be constant. The cooling was effected by natural convection and radiation to the surroundings. The condenser side was a painted black surface with emissivity, $\varepsilon = 1$. An extended 2D representation of the heat input has been utilized, based on a hybrid experimental and numerical heat input model proposed by Carbajal et al. [18]. The heat pipe wick was assumed to be a homogeneous and isotropic porous medium (constant porosity and permeability). The dissipation effects were neglected. Constant viscosity was assumed for the fluid medium, along with constant material properties for the solid wall.

2.2. Governing equations

The governing equations were written in the conservative form [19].

2.2.1. The continuity equation

Incompressible flow was assumed in the wick.

$$\nabla \cdot \vec{V} = 0 \tag{1}$$

The continuity equation for the vapor is given as follow:

$$\frac{\partial \rho_v}{\partial t} + \nabla \cdot \left(\rho_v \vec{V}\right) = 0 \tag{2}$$

2.2.2. The momentum equation

In the generally applicable form, for the vapor core and the wick, the momentum equation is given as follows:

$$\varphi^{-1}\left[\frac{\partial(\rho\vec{V})}{\partial t} + \nabla\cdot(\rho\vec{V}\vec{V})\right] = \rho\vec{g} - \nabla p + \frac{\mu}{\varphi}\nabla^2\vec{V} - \frac{\mu}{K}\vec{V} - \frac{C_E\rho_v}{K^{0.5}}|\vec{V}|\vec{V} - F_B \tag{3}$$

The expression F_B, on the right hand side of Eq. (3) represents the differential form of the Young–Laplace equation. This expression computes the pumping effects of the porous medium [18]. It is defined as follows:

$$F_B = \frac{2\sigma\cos\theta}{r^2}\nabla r \tag{4}$$

In the case of the vapor core, this equation is simplified as the porosity (φ) becomes 1, the permeability approaches infinity ($K \to \infty$), and $F_B = 0$.

2.2.3. The energy equation

The energy equation, under the assumption of no heat dissipation may be written in the form:

$$\frac{\partial}{\partial t}(c_m T) + \nabla\cdot(c\vec{V}T) = \nabla\cdot(k_{eff}\nabla T) \tag{5}$$

Table 1 summarizes the governing equations and their corresponding parameters for the solid plate, wick and vapor core. In the present analysis metal foam was used as the wick material. The state equation for an ideal gas was applied to the vapor:

$$P = \rho_v R T \tag{6}$$

2.3. The boundary and initial conditions

Initially the liquid and vapor phases were at rest and the system was in thermal equilibrium with the ambient surroundings. During operation, the velocity at the liquid vapor interface in m/s (interface of the wick and the vapor core) is computed according to Eq. (7), [18]:

$$u_i = \frac{2\hat{\sigma}}{2-\hat{\sigma}}\left(\frac{1}{2\pi R T_v}\right)^{1/2}\frac{\Delta T}{T_v}[2449100 - 2800(T_v - 273)] \tag{7}$$

Eq. (7) was incorporated into the energy balance at the liquid–vapor interface; as well as the Clausius–Clapeyron equation to compute the pressure at the liquid–vapor interface.

The unknown heat flux input on the evaporator side of the panel was modeled by the expression given in Eq. (8),

Table 1
The governing equations and parameters of the solid, wick and vapor phase

The energy equation $\frac{\partial}{\partial t(c_m T)} + \nabla \cdot (\rho C \vec{V} T) = \nabla \cdot (k_{eff} \nabla T)$	Solid	$k_{eff} = k_s, c_m = (\rho C)_s, \vec{V} = 0$
	Wick	$k_{eff} = \Lambda[\varphi k_f + (1-\varphi)k_s] + (1-\Lambda)\left[\frac{\varphi}{K_f} + \frac{(1+\varphi)}{k_s}\right]^{-1}$ $C_m = (1-\varphi)(\rho C)_s + \varphi(\rho C)_f$
	Vapor	$k_{eff} = k_v,\ c_m = (\rho C)_v$
The momentum equation $\varphi^{-1}\left[\frac{\partial(\rho\vec{V})}{\partial t} + \nabla \cdot (\rho \vec{V}\vec{V})\right] = \rho\vec{g} - \nabla p + \frac{\mu}{\varphi}\nabla^2\vec{V} - \frac{\mu}{K}\vec{V} - \frac{C_E \rho_v}{K^{0.5}}\lvert\vec{V}\rvert\vec{V} - F_B$	Wick	$0 < \varphi < 1$
	Vapor	$\varphi = 1,\ K \to \infty,\ F_B = 0$
The mass conservation $\frac{\partial \rho}{\partial t} + \nabla \cdot \vec{V} = 0$	Wick	$\nabla \cdot \vec{V} = 0$
	Vapor	$\frac{\partial \rho}{\partial t} + \nabla \cdot \vec{V} = 0$

corresponding to a hybrid numerical–experimental analysis [18]:

$$q''(x=0,y,z) = C_1\left[1 - \exp\left\{-\left(\frac{Y-y}{Y/2}\right)\right\} + C_2\right] \times \left[1 - \exp\left\{-\left(\frac{Z-z}{Z/2}\right)\right\} + C_3\right] \quad (8)$$

Here, C_1, C_2 and C_3 are constants, and Y and Z are half the height (H) and the length (L) of the flat heat pipe (or solid plate), respectively. In the present analysis, the heat flux input was symmetric about the z-axis ($C_2 = C_3 = e^{-2}$). Fig. 2 depicts the net non-uniform heat flux input distribution caused by a propane torch impinging perpendicularly on the front side, described by Eq. (8). It can be noticed that the peak of the net heat flux input coincides with the center of the front plate.

The heat flux at the condenser side of the plate was computed as follows:

$$q''(x=W,y,z) = h(T - T_\infty) + \sigma_R \varepsilon (T^4 - T_\infty^4) \quad (9)$$

At the initial condition it was assumed that the saturation condition prevailed in the working fluid at its corresponding initial temperature, and that the fluid was at rest. Carbajal et al. [18] have presented an extensive discussion and details of the boundary and initial conditions used in the present analysis.

Fig. 3 shows the thermal resistance across the solid plate and across the flat heat pipe. It is clear from this figure that the solid plate (Fig. 3a) will experience a smaller resistance

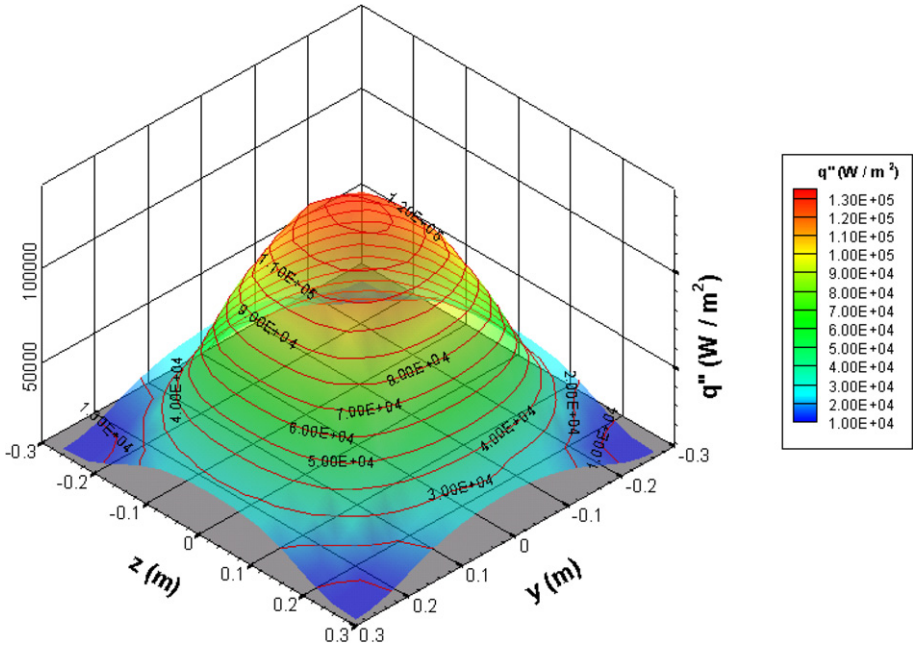

Fig. 2. The heat flux distribution on the front panel.

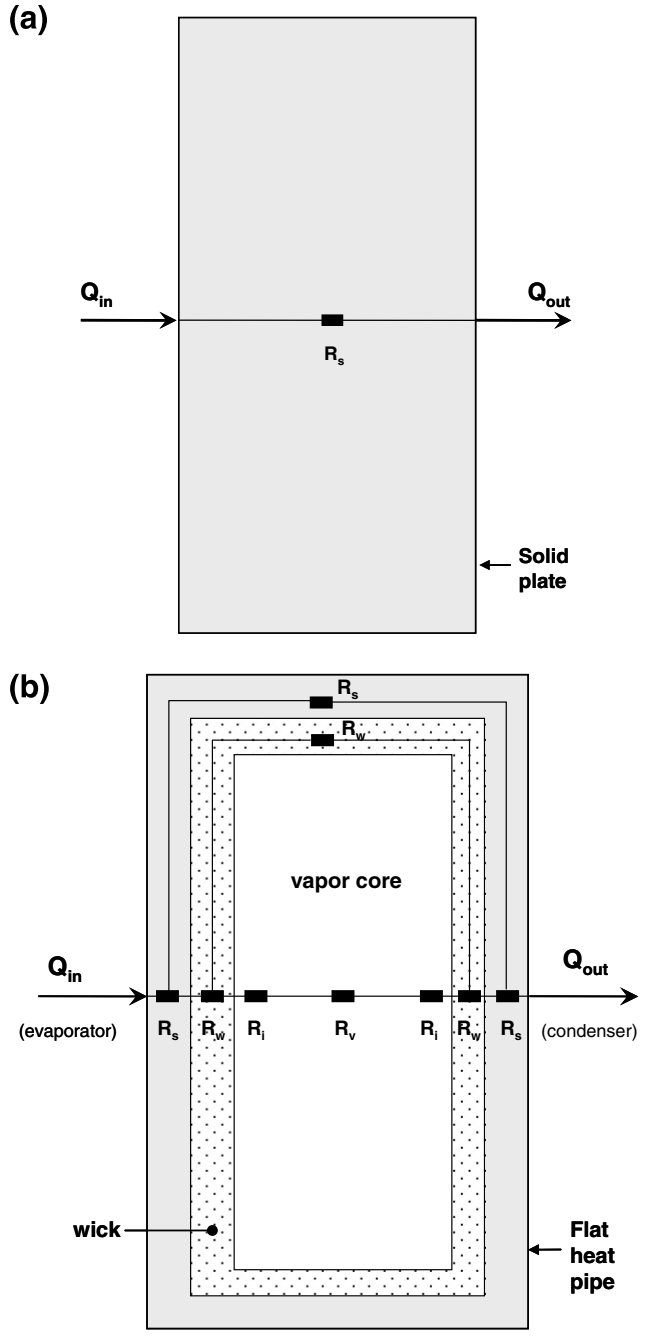

Fig. 3. Thermal resistances across (a) solid plate and (b) flat heat pipe.

to heat transfer. The flat heat pipe Fig. 3b is subjected to several thermal resistances. As a consequence the solid plate will cause a smaller temperature drop along the x direction than the flat heat pipe. The liquid saturated wick and the liquid vapor interface are responsible for significant thermal resistance in the flat heat pipe. Thus, in order to minimize the thermal resistance, careful attention must be paid to the selection of the wick thickness and the latent heat of vaporization of the working fluid. The thermal resistances shown in Fig. 3 are those of the front wall ($\mathbf{R}_s$), the saturated porous medium ($\mathbf{R}_w$), the liquid vapor interface ($\mathbf{R}_i$), and the vapor core ($\mathbf{R}_v$).

During the transient process the flat heat pipe experiences an energy imbalance between the heat input (Q_{in}) and the heat rejected (Q_{out}). Initially a fraction of the total heat input is stored in the body of the heat pipe and another fraction is released to the ambient by natural convection and radiative effects. The following expression represents the transient process:

$$1 - \frac{Q_{out}}{Q_{in}} > 0 \tag{10}$$

The transient process will cause an entropy generation in the system, so the overall thermal efficiency of the system is poor at this early stage of the process. The entropy generation is associated with the presence of different temperature gradients in the system. The total mass of the system composed of the solid wall, wick and vapor core will increase the thermal capacitance of the system. A system with a considerable amount of mass will respond slowly to the heat transfer process than a lighter system. So systems with large amounts of mass will take a long time to reach their corresponding steady state. In the present study the early transient process in a flat heat pipe was investigated, as the system being considered is of large mass, and the heat input was applied for a short period of time.

2.4. Solution method

A quasi-3D approach was used to solve the problem, such that the 3D effects were captured to the extent possible, all the while not making the solution procedure unreasonably complex and time consuming. In order to simplify the analysis, the flat heat pipe was split into several equidistant x–y planes along the z-direction. As a result of the symmetry of the heat input about the z-axis, the computational domain was reduced to only one quarter of the entire flat heat pipe. The governing equations were sequentially solved at various locations along the z-direction, with the boundary and initial conditions similar to those presented by Carbajal et al. [18]. Inspired by the successful use of the finite volume method in solving a variety of problems related with fluid flow and heat transfer [20–22]; an explicit finite volume numerical approach was applied, suppressing the undesired instabilities in the vapor core by the use of appropriate under-relaxation parameters [23]. Meshes of 10×80, 20×100, 40×120, 80×140 were tested. The final grid of 40×120 was selected based on the grid independence test, where successive grid refinement did not give deviations larger than 0.32%.

3. Results and discussion

A quasi-3D numerical model was developed to analyze the flat heat pipe, which is capable of predicting the temperature distributions, among other field variables. Due to the symmetry of the heat flux distribution in the x–y and x–z planes at the center of the FHP, the domain of the problem formulation was restricted to one quarter of

the flat heat pipe, as shown in Fig. 4. The analytical expression for the heat flux distribution proposed by Carbajal et al. [18] was used in the analysis. Using a numerical code developed in Fortran 90 the analysis was performed on different x–y planes, on various locations along the z-direction. The limitation in this analysis is the formulation which neglects the heat flux and the fluid flow perpendicular to the x–y plane; however, the results suggest that this limitation does not significantly affect the calculation. To demonstrate the potential capability of the flat heat pipe as a thermal spreader, the results were compared with those from a numerical analysis performed on a solid aluminum plate subjected to the same heat flux input, initial and boundary conditions.

Contour plots of the numerical results on the velocity field in the vapor core are presented in Fig. 5. Figs. 6 and 7 give the transient temperature response on the back side of the solid aluminum plate and flat heat pipe, respectively, in order to demonstrate the potential of the heat pipe as a heat spreader.

In heat pipes, evaporation and condensation are the two fundamental processes that make possible the transfer of energy from the heat source (or evaporator) to the remote heat sink (or condenser). At the evaporator, a large amount of energy is consumed in order to cause the phase change from the liquid state to the vapor state, equivalent to the latent heat of vaporization. The rate of heat rejected at the condenser is influenced by the velocity of the vapor field and the latent heat. Consequently the local velocities of the vapor affect the rate of the cooling process no matter how small it is.

Fig. 5 shows the contour plot of the velocity distribution at four different locations along the z-direction. The results indicate that the velocity field at the vapor core is affected

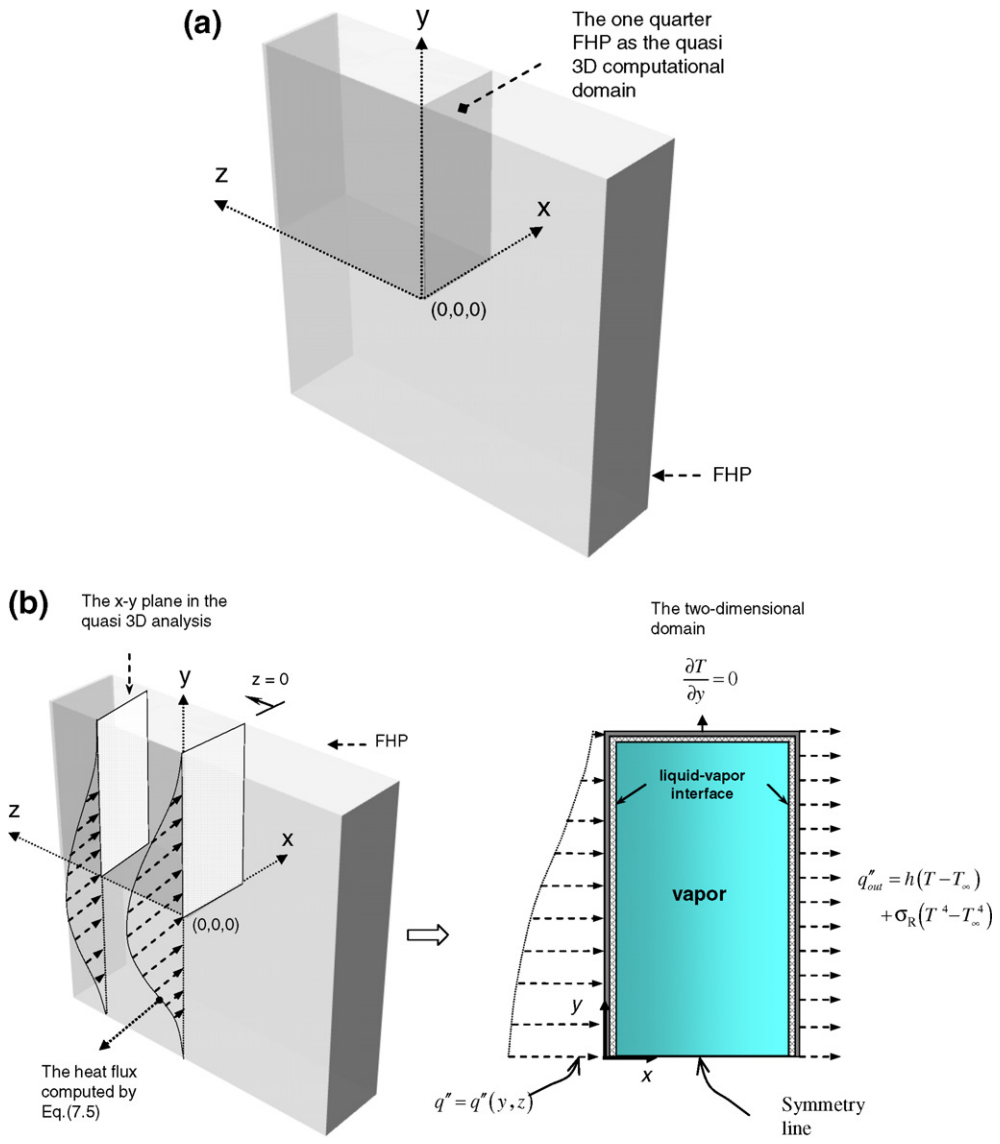

Fig. 4. (a) The FHP computational domain. (b) The heat flux on x–y planes along the z-direction.

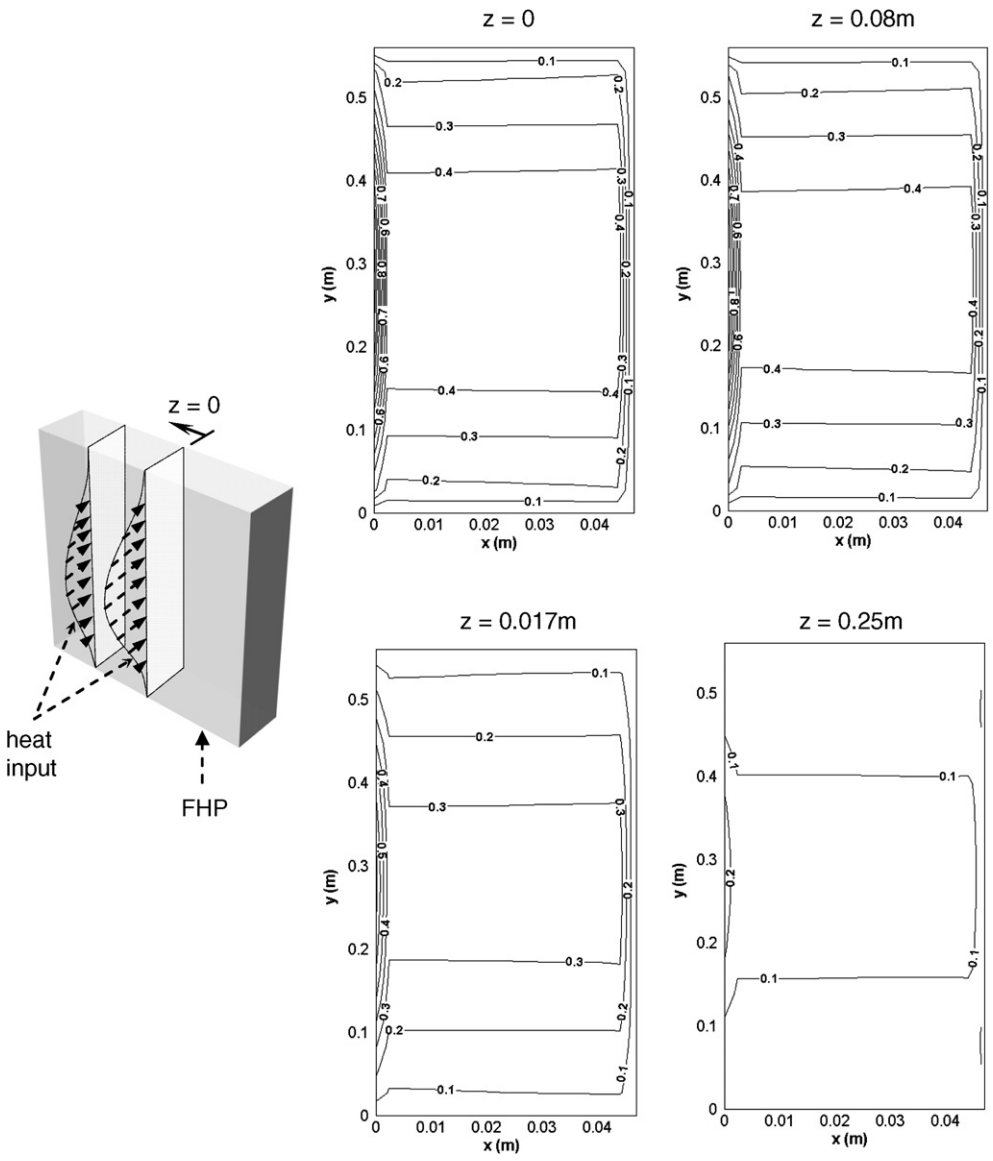

Fig. 5. Contour plots of the velocity distribution in the vapor core in m/s at different z-locations, $t = 30$ s.

by the magnitude of heat input applied at the evaporator. The four x–y planes at four different locations exhibit different velocity fields because the heat input is different at these planes. At $z = 0.00$ m the x–y plane is exposed to the maximum heat flux, which results in the largest velocity distribution in the vapor core. As the analysis is extended to different locations away from the origin ($z = 0.08$ m, 0.17 m, and 0.25 m), the velocity field in the vapor core becomes less intense. As the heat flux is a function of the y and z coordinates, the vaporization rate at the evaporator is subsequently influenced by the location of the input heat flux, thus affecting the local vapor velocity in the vapor core.

In order to demonstrate the potential of the flat heat pipe as a heat spreader, a comparison was performed with computational results on a solid aluminum plate, for similar heat input and boundary conditions. The temperature distribution across the x–y plane of the solid aluminum plate and the flat heat pipe are presented in Figs. 6 and 7. According to these results, the heat pipe is able to generate a more uniform temperature distribution across the x–y plane than the solid plate which is subjected to pure conduction. These results also indicate that pure conduction is not capable of distributing a non-uniform heat input given at the front panel uniformly on the back side of the plate. The temperature distributions at the back side of the aluminum plate and the flat heat pipe are presented in Figs. 8 and 9.

Fig. 8 illustrates the transient temperature response at the back side of the aluminum plate, corresponding to the application of a constant non-uniform heat flux at the front side, at elapsed times of 1, 10, 20, 30 and 40 s. On comparing this with the temperature response of the flat heat pipe at corresponding time increments of 1,

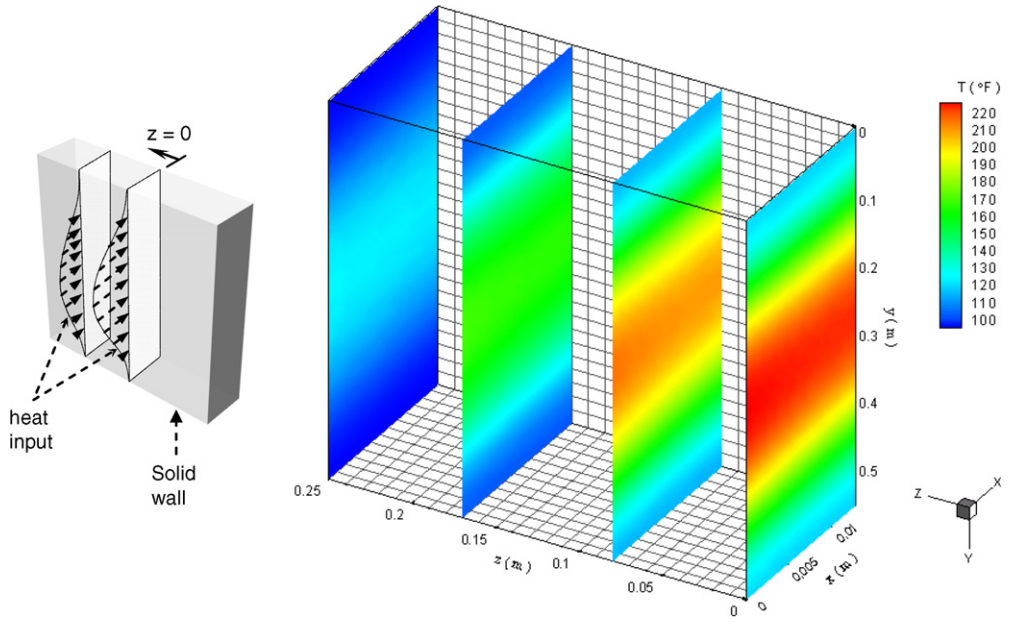

Fig. 6. Temperature distribution across a solid aluminum plate at different z-locations, $t = 20$ s.

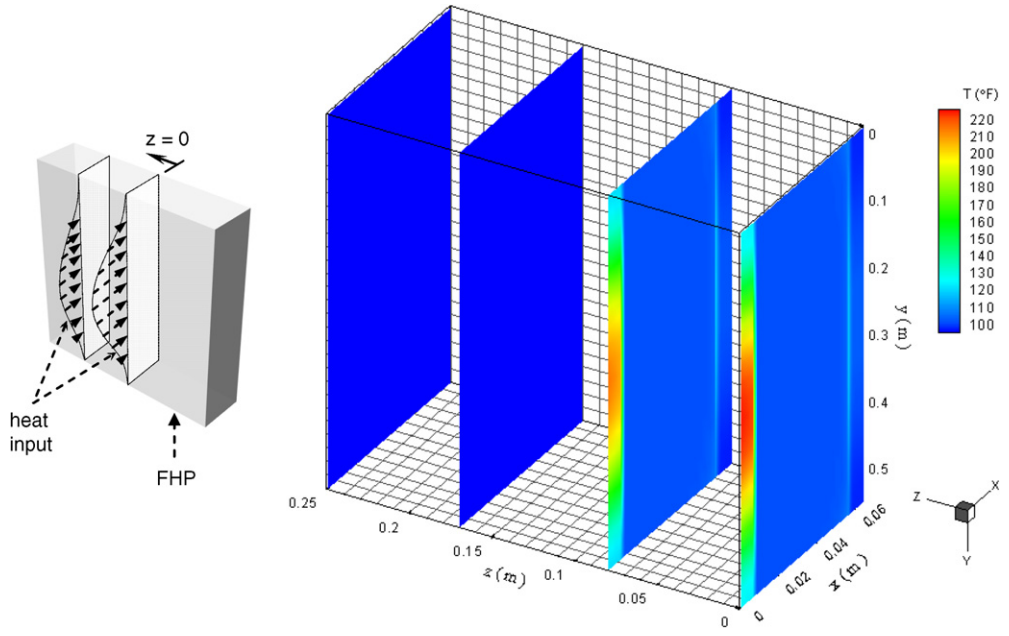

Fig. 7. Temperature distribution across a flat heat pipe at different z-locations, $t = 20$ s.

10, 20, 30 and 40 s, shown in Fig. 9, it is obvious that the temperature distribution at the back side has become more uniform as time proceeds. In other words, the results shown in Figs. 8 and 9 indicate the slower response of the soild plate to spread heat on the condenser compared to the flat heat pipe (thermal spreader). The evaporation and condensation processes in the vapor core of the heat pipe thermal spreader causes the rapid transport of energy from the evaporator to the condenser side, and spreads it out because of the liquid flow through the wick structure. As the heat transport rate is influenced by the latent heat of the working fluid, and as the phase change process involves large quantities of energy, the heat pipe is much more effective than the pure conduction mechanism.

The vaporization and condensation processes inside the flat heat pipe spread the heat more uniformly throughout the system, as obvious from the results presented. As a consequence, no region of temperature concentration (hot spot) is produced at the back side of the sandwich panel. The uniform temperature distribution observed on the

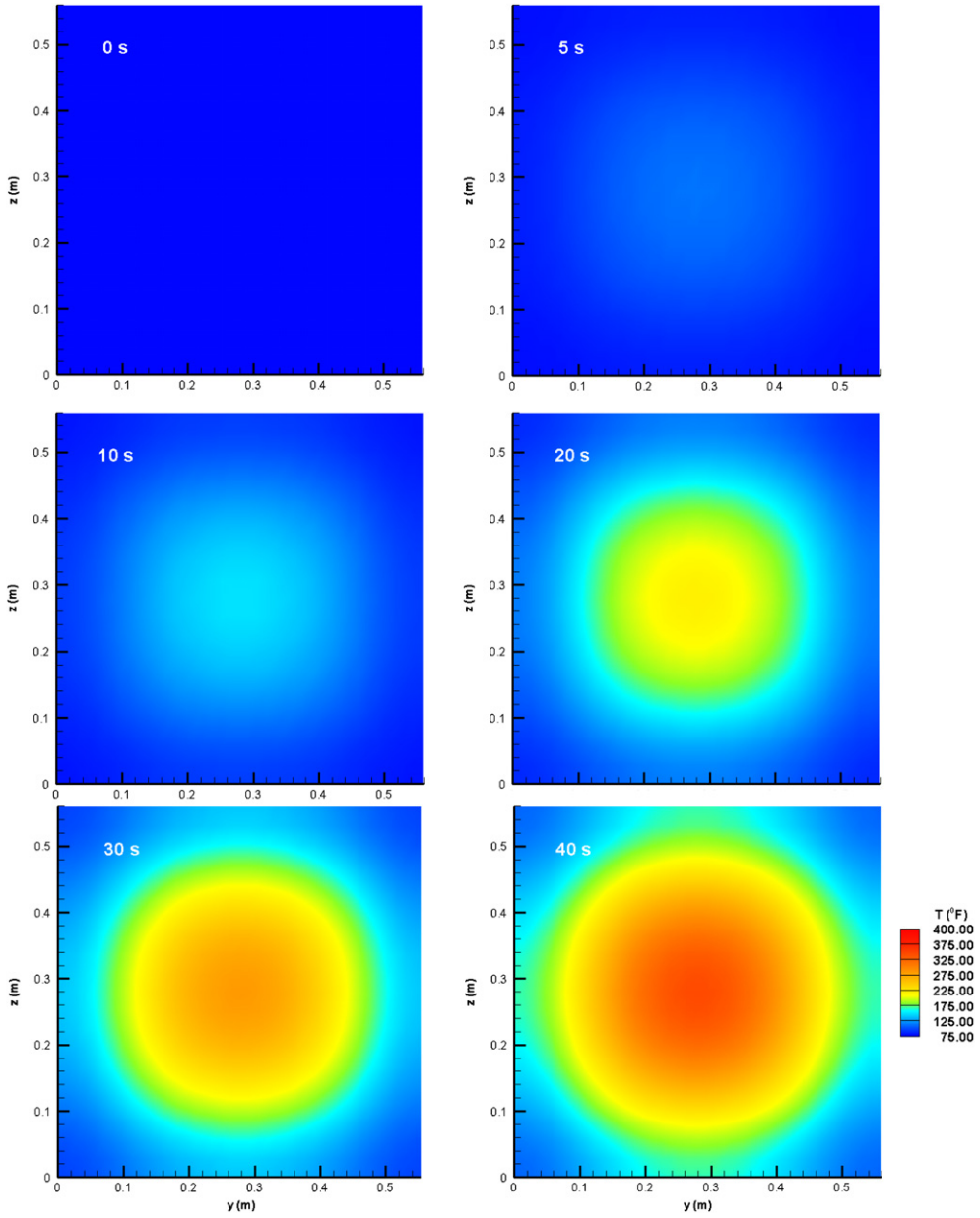

Fig. 8. Temperature distribution on the condenser side of the solid aluminum plate – results from numerical computations.

back side of the panel makes the flat heat pipe a desired heat spreading device which can dissipate heat very effectively as the whole surface area on the back side can take part in a heat exchange process between the metal surface which is generally at a moderately high temperature than a cooling fluid flow.

4. Conclusion

A quasi-3D numerical analysis was performed to obtain the temperature distribution on the back side of a flat heat pipe thermal spreader, while a concentrated heat load was applied to the front panel. The model incorporates the phase change mechanisms at the liquid and vapor interface inside the heat pipe, and considers combined convective and radiative heat transfer modes at the back side of the heat spreader. It was demonstrated that the flat heat pipe works as a thermal spreader, with a much more uniform temperature distribution at the condenser side, than a solid aluminum plate with comparable heat input and boundary conditions. The applicability of the flat plate heat pipe as a heat spreader is determined and discussed in detail, based on the numerical results.

Acknowledgements

The authors acknowledge the joint support from the Defense Advanced Research Projects Agency and the Office of Naval Research under Grant No. N00014010454

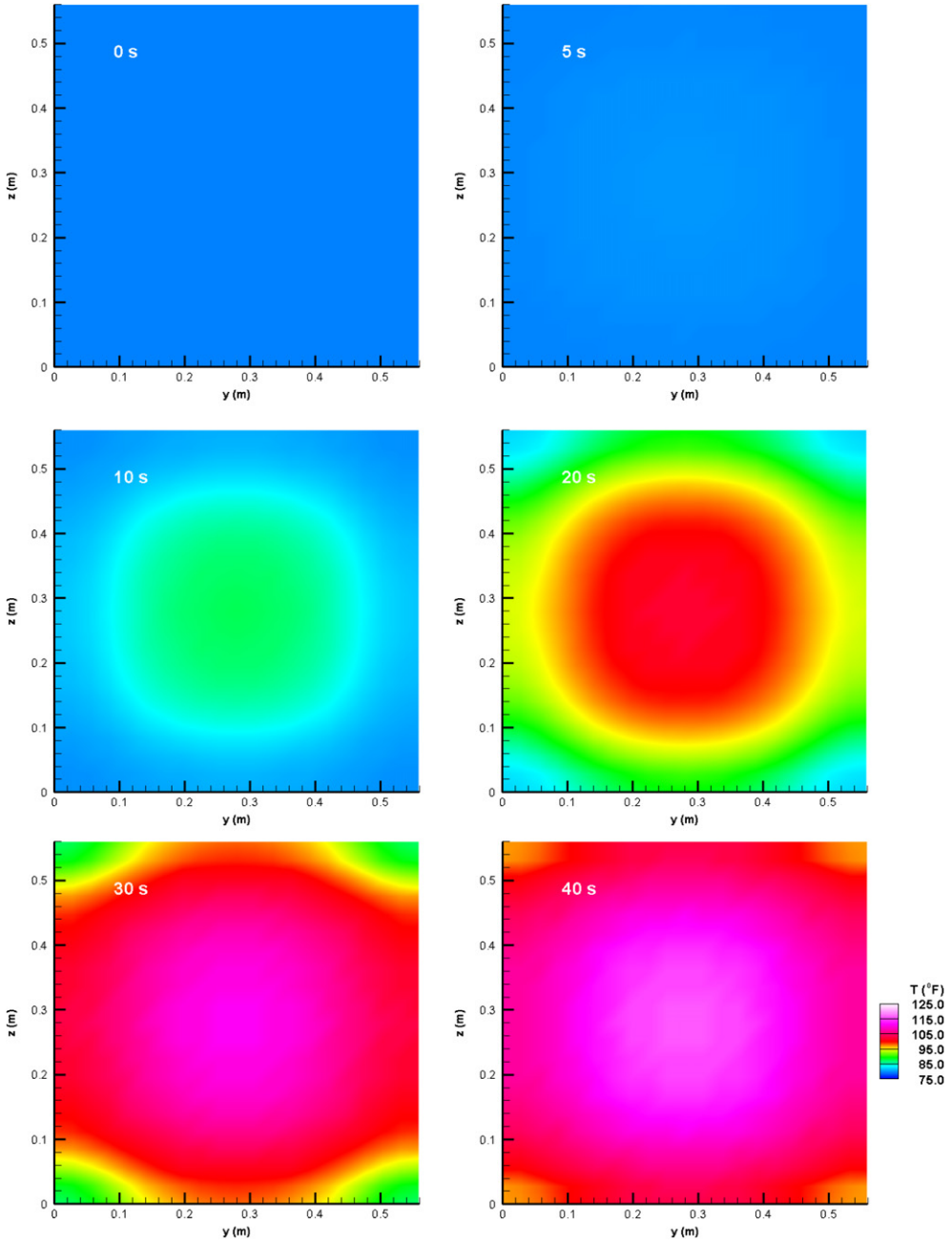

Fig. 9. The temperature distribution on the condenser side of the flat heat pipe – results from numerical computations.

and the support of the National Science Foundation through Grant No. CTS-0312848.

References

[1] R.S. Gaugler, Heat transfer device, U.S. Patent No. 2,350,348, 1944.
[2] A. Basiulis, C.M. Eallonardo, B.M. Kendall, Heat-pipe system for space shuttle traveling wave tube amplifier, in: AIAA Eighth Thermophysics Conference, Palm Springs, CA, 1973, pp. 431–444.
[3] C.J. Camarda, Aerothermal test of a heat-pipe-cooled leading edge at mach 7, NASA Technical Paper 1320, 1978.
[4] F. Edelstein, Transverse flat plate heat pipe experiment, in: Proceedings of the Third International Heat Pipe Conference, Palo Alto, CA, 1978.
[5] A. Basiulis, C.A. Torrance, C. Camarda, Design, fabrication and testing of liquid metal heat-pipe sandwich panels, in: AIAA/ASME Third Joint Thermophysics, Fluids, Plasma and Heat Transfer Conference, St. Louis, MO, 1982.
[6] K.C. Cheng, Applications of heat pipes and thermosyphons in cold regions, in: Seventh International Heat Pipe Conference, Minsk, USSR, 1990.
[7] A. Basiulis, C.P. Minning, Improved reliability of electronic circuits through the use of heat pipes, in: 37th National Aerospace and Electronic Conference, Dayton, OH, 1985.
[8] J. Wei, K. Hijikata, T. Inoue, Fin efficiency enhancement using a gravity – assisted planar heat pipe, Int. J. Heat Mass Tr. 40 (5) (1997) 1045–1051.
[9] J.S. Go, Quantitative thermal performance evaluation of a cost-effective vapor chamber heat sink containing a metal-etched

microwick structure for advanced microprocessor cooling, Sensor. Actuat. A 121 (2005) 549–556.
[10] W.S. Chang, G.T. Colwell, Mathematical modeling of the transient operating characteristics of a low-temperature heat pipe, Numer. Heat Tr. 8 (1985) 169–186.
[11] J.H. Ambrose, L.C. Chow, Detailed model for transient liquid flow in heat pipe wicks, J. Thermophys. 5 (4) (1991) 532–538.
[12] M. Chang, L.C. Chow, Transient response of liquid metal heat pipes – a comparison of numerical and experimental results, in: Proceedings of the Eighth International Heat Pipe Conference, Beijing, China, 1992.
[13] J.M. Tournier, M.S. El-Genk, A heat pipe transient analysis model, Int. J. Heat Mass Tr. 37 (5) (1994) 753–762.
[14] J.M. Tournier, M.S. El-Genk, Transient analysis of the start-up of a water heat pipe from a frozen state, Numer. Heat Tr. A 28 (5) (1995) 461–486.
[15] Z.J. Zuo, A. Faghri, Boundary element approach to transient heat pipe analysis, Numer. Heat Tr. A 32 (3) (1997) 205–220.
[16] C.B. Sobhan, S.V. Garimella, V.V. Unnikrishnan, A computational model for the transient analysis of flat heat pipe, in: Thermomechanical Phenomena in Electronic Systems – Proceedings of the Intersociety Conference, vol. 2, 2000, pp. 106–113.
[17] U. Vadakkan, J.Y. Murthy, S.V. Garimella, Transient analysis of flat heat pipes, in: Proceedings of the 2003 ASME Summer Heat Transfer Conference, HT2003-47349, Las Vegas, NV, 2003, pp. 1–11.
[18] G. Carbajal, C.B. Sobhan, G.P. Peterson, D.T. Queheillalt, H.N.G. Wadley, Thermal response of a flat heat pipe sandwich structure to a localized heat flux, Int. J. Heat Mass Tran. 49 (2006) 4070–4081.
[19] G. Carbajal, C.B. Sobhan, G.P. Peterson, Dimensionless governing equations for the vapor and liquid flow analysis of heat pipes, J. Thermophys. Heat Tr. 20 (1) (2006) 140–144.
[20] D. Pan, C. Lu, Upwind finite-volume method for natural and forced convection, Numer. Heat Tr. B–Fund. 26 (2) (1994) 207–224.
[21] S. Muzaferija, M. Peric, Computation of free-surface flows using the finite volume method and moving grid, Numer. Heat Tr. B–Fund. 32 (4) (1997) 369–384.
[22] J.C. Chai, One-dimensional transient radiation heat transfer modeling using a finite volume method, Numer. Heat Tr. B–Fund. 44 (2) (1997) 187–208.
[23] G. Carbajal, C.B. Sobhan, G.P. Peterson, Numerical study of heat pipe heat spreader with large periodic heat inputs, J. Thermophys. Heat Tr. 20 (4) (2006) 835–841.